Splashing from drop impact into a deep pool: multiplicity of jets and the failure of conventional scaling

L. V. Zhang[1], J. Toole[1]†, K. Fezzaa[2], R. D. Deegan[1]‡

[1]Department of Physics & Center for the Study of Complex Systems, University of Michigan, Ann Arbor, MI 48109 USA

[2]X-Ray Science Division, Argonne National Laboratory, Argonne, IL 60439, USA

(Received 23 May 2012)

We report high-speed optical and X-ray observations of jets formed during the impact of a drop with a deep pool of the same liquid. We show that a scaling which relies entirely on liquid properties, as is conventionally employed, is insufficient to determine the threshold for splashing. In order to determine if the gas properties could account for this deficit, we conducted experiments with different surrounding gases. We find that the splashing threshold depends on the gas's dynamic viscosity, but not its density. We argue that these results are consistent with a thickening of the ejecta caused by the bubble trapped on impact between the drop and the pool. We also show that drop impact can generate a third jet, distinct from the lamella and the ejecta, that produces secondary droplets of an intermediate size.

1. Introduction

The primary components of a splash from the impact of a drop with a liquid layer have been known for over hundred years. Worthington (1882) showed that on impact a cylindrically-symmetric jet forms, grows, and disintegrates into a spray of secondary droplets. Nonetheless, many basic details of this process remain obscure. How many jets are there? What sets their size and speed? What is the origin of the symmetry breaking instability? What is the size distribution of droplets that comprise the splash? In order to investigate these issues we used high-speed X-ray and visible imaging to probe one of the simplest splashing scenarios: normal incidence of a single spherical drop onto a deep pool of the same liquid.

That there is more than one jet was first discovered in numerical simulations (Weiss & Yarin 1999) and later confirmed by experiments (Thoroddsen 2002). Weiss & Yarin (1999) showed that upon impact a thin fast jet was ejected from the neck between the drop and the incident pool. Here we call this jet the *ejecta*, the jet observed by Worthington – which is slower, emerges later, and produces the so-called crown splash – the *lamella*, and any production of secondary droplets from the disintegration of a jet *splashing*. Zhang *et al.* (2012) showed that the lamella and ejecta are separate entities at high Reynolds number but join into a single jet at low Reynolds number. Here we show that there is at least one more jet.

The question of the size distribution of secondary droplets is intimately tied to the

† Present address: Engineering systems division, MIT , Cambridge, MA 02139, USA
‡ Email address for correspondence: rddeegan@umich.edu

	Fluid	Viscosity (cp)	Density (g/cm^3)	Surface tension (dyne/cm)	Drop Diameter (cm)
silicone oil	SO	0.49	0.759	15.7	0.176
pyridine	PYR	0.88	0.957	38.0	0.184
glycerol-water solution	GW	1.30	1.038	66.0	0.224

TABLE 1. Physical properties of experimental fluids at 21 ^{o}C.

Gas	Viscosity (centipoise)	Density (10^{-3} g/cm^3)
air	1.849×10^{-2}	1.1840
helium	1.985×10^{-2}	0.16353
sulfur hexafluoride	1.535×10^{-2}	6.0380

TABLE 2. Physical properties of experimental gases at 25 ^{o}C (Lemmon *et al.* 2010).

number of jets, their size, and their instabilities. In the course of determining these parameters we discovered that the standard parameterization based on the Reynolds and Weber number is insufficient to account for the splashing threshold. Furthermore, we identified the onset of the instability that leads to splashing and found that neither can this threshold be account for with only the Reynolds and Weber number. We investigated the dependence on the surrounding gas as a potential source of these discrepancies. Our experiments show that the instability threshold is sensitive to the gas's dynamic viscosity, but not its density, unlike the dry drop impact case (Xu *et al.* 2005; Xu 2010).

2. Experimental Setup

In our experiments a drop fell through a fixed height on to a deep pool of the same liquid. We used high speed video with visible light and X-rays to observe the ensuing dynamics. Our experiments were conducted with a low-viscosity silicone oil (nominally 0.65 cSt, Clearco), a 11.1:100 v/v glycerol-water mixture, and pyridine (Sigma-Aldrich). We measured the kinematic viscosity of these fluids with a Cannon-Fenske routine viscometer, their density with a Gay-Lussac bottle, and their surface tension with a Wilhelmy plate apparatus. These properties are listed in Table 1. These particular liquids were chosen because their physical properties together with the size of the drops they produced yielded the same Ohnesorge number $Oh = \eta/\sqrt{\gamma\rho D}$ where η is the dynamic viscosity, γ is the surface tension, ρ is the density, and D is the drop diameter. All experiments were done at ambient temperature: 21 ± 1 ^{o}C for the visible light measurements and 22.3 ± 0.2 ^{o}C for the X-ray measurements. We assumed that the minor variation of the physical parameters between different experiments due to temperature differences was negligible.

While the physical properties of the fluid are fixed, the diameter of the drop depends additionally on the method of production. Each drop was formed on the tip of an electrically grounded sewing needle, fed by a hypodermic needle connected to a reservoir or to a syringe pump when better control of the interval between drops was needed. The sewing needle/hypodermic needle combination is superior to a hypodermic needle by itself because the conical tip of the needle produces drops with less surface oscillations,

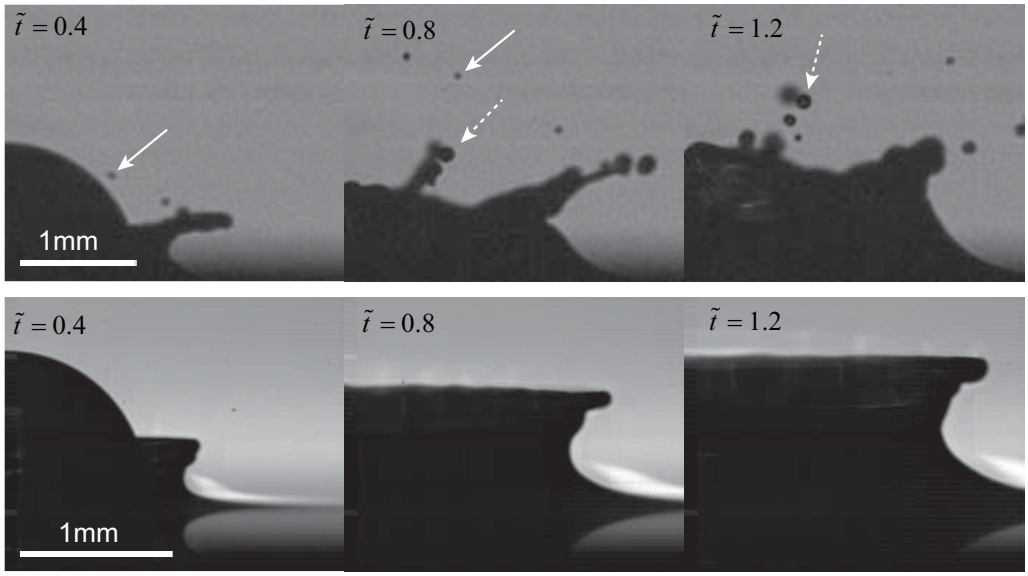

FIGURE 1. Optical images of drop impact with a glycerol-water mixture (above) at $Re = 5450$, $We = 330$ and a low viscosity silicone oil (below) at $Re = 5330$, $We = 340$ at the indicated normalized time $\tilde{t} = Ut/D$. Despite almost identical experimental conditions the event on the top produces a splash of microdroplets (solid arrow) and intermediate droplets (dashed arrow), while the one below does no secondary droplets. The images are scaled to equal drop diameters ($D = 0.22$ cm and $D = 0.18$ cm for the GW and SO, respectively) (i.e. to the same non-dimensional length scale).

	X-Ray method	Optical method
GW	3420	3730
PYR	n/a	4030
SO	4760	5160

TABLE 3. *Re* threshold in air as determined with X-ray and optical imaging.

more uniform drop diameters, and less variability of the impact site. The diameter of the drops for each particular fluid is listed in Table 1; variation of the diameter was less than 3% and was primarily due to minor variations in the size of different sewing needles. The drop diameters were typically about 2 mm and showed minor distortion due to air drag when falling through air; for the largest fall heights the horizontal width of the drop was 3% bigger than than its vertical height.

The pool on which the drop impacted was formed in a circular container 10 cm wide and 5 cm deep. Experiments with smaller containers (order 1 cm) did not alter the results, and thus the horizontal and vertical extents of the pool were effectively infinite. Impact speeds ranged from 1.2-3.5ms/s. The interval between successive impacts was kept long to allow waves from the previous impact to dissipate.

The surrounding gas was changed by enclosing the system within a plastic bag (X-ray measurements) or a chamber (visible measurements) and pushing out the air with either helium or sulfur hexafluoride (SF6). A slow flow of the replacement gas was maintained

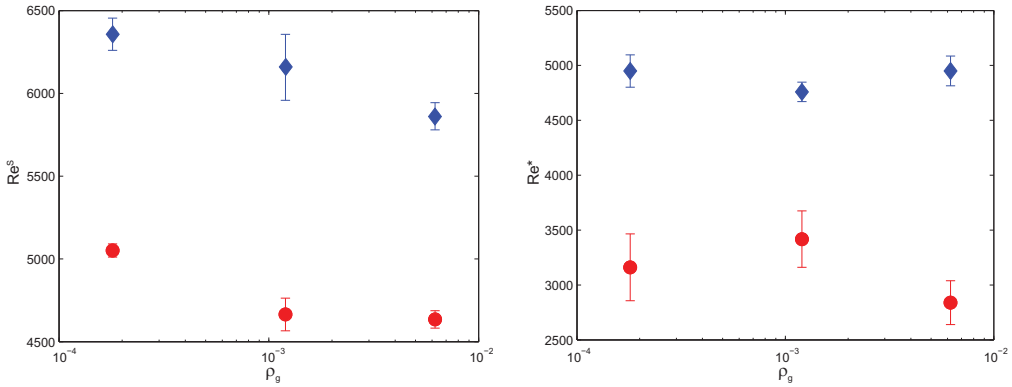

FIGURE 2. Left: Reynolds number threshold for onset of splashing, defined as the appearance of secondary droplets, in GW (circles) and SO (diamonds) versus density of the surrounding gas. These data correspond to helium, air and SF_6 going from left to right. Right: Reynolds number threshold for onset of instability in GW (circles) and SO (diamonds) versus density of the surrounding gas. Note: symmetry breaking criterion gives a lower threshold than splashing criterion because at lower values of Re the ejecta is reabsorbed before the instability produces fragmentation.

throughout the experiments and vented through a small orifice at the bottom or top in case of helium or SF_6, respectively, to ensure a pure environment.

Our visible light measurements were obtained with a high speed video camera (Phantom v11, Vision Research) fitted with a 1.4-9.0X zoom lens (Navitar 6000) or a 60 mm f/2.8 macro lens (Nikon). Our X-Ray measurements were conducted at the Advanced Photon Source at Argonne National Laboratory using a phase contrast technique (Fezzaa & Wang 2008). The X-rays traversed horizontally through the splash and were imaged on a scintillator crystal with a high speed video camera (SA1.1, Photron). The X-ray data consisted of gray scale images in which greater absorption produced darker shades. In addition, the phase contrast technique highlights the interface of the fluid parallel to the beam with a dark or light halo. The advantage of X-ray imaging is that it reveals the structure of a splash that would be obscured in visible light by reflections and refraction from the interfaces and out-of-focus features.

3. Results & Discussion

3.1. *Inadequacy of conventional scaling*

The impact of a drop with a layer of the same fluid is conventionally described by six physical quantities: the impact velocity U, the drop diameter D or radius R, the fluid's properties (γ, ρ, η), and the acceleration due to gravity g. Non-dimensionalizing time with D/U and length with D yields a parametrization in terms of the Weber number $We = \rho DU^2/\gamma$, Reynolds number $Re = \rho DU/\eta$, and Froude number $Fr = U^2/gD$. Hereafter we refer to this set of non-dimensional numbers as the conventional parameterization.

Experiments almost universally ignore the Froude number dependence (see e.g. Cossali *et al.* 1997; Rioboo *et al.* 2003; Deegan *et al.* 2008) because the acceleration due to gravity is negligible on the timescale of a splash. The conventional parameterization also neglects the surrounding gas based on the low density ρ_g and low dynamic viscosity η_g of the gas relative to those of the liquid: typically $\rho_g/\rho \approx 10^{-3}$ and $\eta_g/\eta \approx 10^{-2}$.

We tested the conventional parametrization by observing the qualitative character of

splashes from drop impact on a deep pool of the same liquid with three different fluids at the same We and Re number. For any particular fluid $We^{1/2} = Oh \cdot Re$. The fluids in our experiment (SO: silicone oil; GW: glycerol-water mixture; PYR: pyridine) had the same $Oh = 3.4 \times 10^{-3}$. Therefore, experiments with one fluid at any particular combination (We, Re) could be repeated with the other two fluids. If We and Re do indeed provide a complete specification as expected from the conventional parameterization, experiments with any of the three fluids ought to be identical at the same Re. (Given that in our experiments $We = Oh^2 \cdot Re^2$ and Oh is a constant, Re is sufficient to specify the experiment; hereafter we only report Re).

Figure 1 shows impact events for GW (above) and SO (below) with almost equal $Re \approx 5400$. The impact in GW produces a splash while the one in SO does not. Moreover, Fig. 2 shows that Re^s, defined as Re at which secondary droplets first appear, is 1500 greater for SO than GW. This discrepancy suggest that the conventional scaling is inadequate.

We find further confirmation of this discrepancy using X-ray imaging. Figure 3 shows the evolution of the ejecta as it emerges from the neck between the drop and the substrate fluid at $Re \approx 4500$. The ejecta for GW displays non-axisymmetric structure which grows into a pronounced corrugation. In contrast, the ejecta from SO is smooth, exhibiting no signs of instability. The instability in GW first appears at $Re = 3400$. We define a new threshold Re^* as the Re at which the ejecta first shows signs of instability. This threshold is plotted for the GW and SO in Fig. 2; again, we find that Re^* for GW is about 1500 lower than for SO.

The splashing threshold is higher than the instability threshold because for $Re^* < Re < Re^s$ the ejecta collides with the bulk of the drop and is reabsorbed before the corrugations develop into droplets. For $Re > Re^s$ the corrugation visible in Fig. 3 breaks-up into the small secondary drops shown in Fig. 1, which we call *microdroplets*; the larger drops, which we call *intermediate droplets* are from a different source; we return to this issue is Section 3.5.

Our X-ray measurement were for GW and SO. To assure ourselves that the observed discrepancy in the fluid was not due to some unrecognized peculiarity of either fluid, we added a third fluid pyridine. Health and safety constraints precluded using pyridine at the Advanced Photon Source. Instead, we employed a visible light method to determine the instability threshold. We focused with a high magnification lens on the contact region of the drop and the pool, and determined the onset the instability from the appearance of a spatial modulation of the light reflected from the rim of the ejecta. As shown in Table 3, the light based detection of the threshold is less sensitive than with X-rays but nonetheless is accurate to better than 10% in the cases for which we could cross-check with X-ray measurements. Table 3 shows that all three fluids exhibit a different instability threshold confirming the threshold shift observed with just two fluids.

The discrepancy in both the splashing and instability thresholds indicates that something is missing from the conventional scaling. We considered whether temperature variations, drag induced vortices in the drop, drag induced deformations of the drop, or oscillations of the drops could account for the discrepancy. We estimated that these effect are at most 1-2% effects which is far too small to account for the observed shifts of 30-40% in the thresholds.

3.2. *Role of the surrounding gas*

There is mounting evidence that the surrounding gas, despite its tenuous physical properties, can qualitatively affect splashing. Notably, for drop impact on a dry substrate Xu *et al.* (2005) found that a reduction of the gas pressure eliminated splashing, and for impact on a wet substrate Thoroddsen *et al.* (2011) showed that drag from the sur-

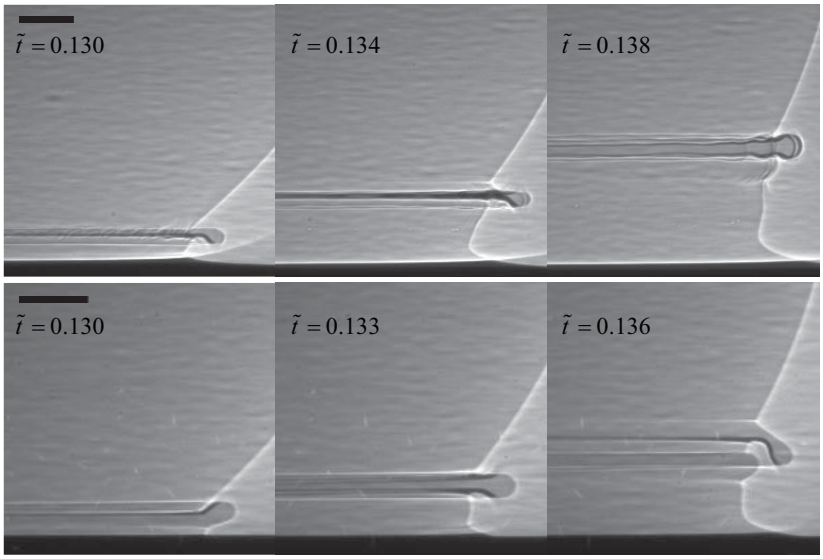

FIGURE 3. Ejecta sheet emerging from the neck connecting a drop (dark gray) and the pool (black) for GW (above) at Re=4540, We=230 and SO (below) at Re=4430, We=230 at the indicated scaled time $\tilde{t} = Ut/D$. The images are scaled to equal drop diameters ($D = 0.22$ cm and $D = 0.18$ cm for the GW and SO, respectively). The scale bars correspond to 100 μm. The X-rays are highly attenuated after traversing the full width of the pool and thus the pool appears as a black band at the bottom of each image.

rounding gas distorts the shape of the lamella, so much so in some cases that the lamella collides with the pool. We thus set about determining if the gas mattered, and if so, which particular property was responsible for the threshold shifts.

Augmenting the conventional parametrization to include the gas introduces two additional dimensionless parameters: the density ratio ρ_g/ρ and the viscosity contrast $\Lambda = \eta_g/\eta$. We examined the effect of these parameters in our experiments. As in air, we determined the lowest Re at which instability appears on the ejecta of GW and SO in two gases (He and SF6) using X-ray imaging. These data are plotted versus gas density in Fig. 2. Despite varying the density by almost two decades, Re^* remains unchanged within the uncertainty of our measurement. We concluded that the gas density is insignificant in determining the onset of the symmetry breaking instability that leads to splashing.

In particular, the result rules out drag from the gas as a potential cause of the threshold shift. The Reynolds number for the ejecta in gas is $Re_j = \rho_g u_j \delta/\eta_g$, where δ and u_j are the ejecta thickness and speed. From measurements $u_j \approx 10U$ Zhang *et al.* (2012) and $\delta \approx 10^{-2}D$, and $Re_j \approx 10^{-2}Re \approx 30$ for typical experimental values of Re. For this value of Re_j the drag is in the inertial regime and proportional to the gas density, but since there was no observable effect of the gas density it follows the drag is not responsible for the shift.

The insensitivity of the instability threshold of the ejecta to the density of the gas shows that if the gas is influencing the experiments then it can only be through a coupling of the gas and fluid that depends exclusively on the ratio of their viscosities. The viscosity of the gases does not change significantly (see Table 2), but the viscosity of the fluids do. Figure 4 shows a plot of the optically determined instability threshold Re^*_{op} versus Λ. These data show that the threshold increases linearly with Λ, i.e. the threshold is shifted upward for a greater viscosity of the gas relative to that of the fluid.

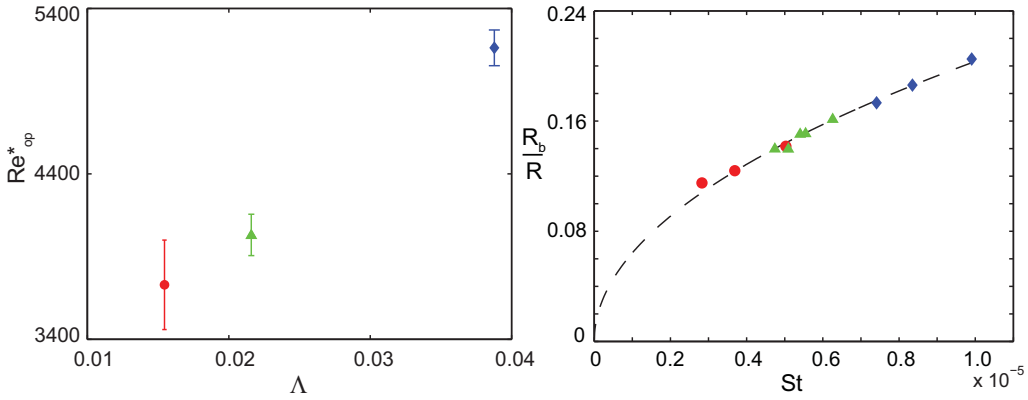

FIGURE 4. Left: Reynolds number threshold determined optically versus viscosity contrast for GW (circle), pyridine (square) and SO (diamond) in air at 1 atm. Right: maximum disk radius normalized by the drop radius versus Stokes number for GW (circles), Pyridine (triangles) and SO (diamonds). The dashed curve is the best fit to power law which yields and exponent of 0.5. Note: R_b increases with Λ.

3.3. *The trapped disk of gas*

The dependence of the threshold on the gas viscosity but not density hints at the action of a low Reynolds number flow in the gas. The most conspicuous location for the latter is the gap between the drop and the pool. Indeed, prior to impact the gas between the drop and the pool must be drained from between the two bodies. Smith *et al.* (2003); Mandre *et al.* (2009); Duchemin & Josserand (2011) showed numerically that in the case of drop impact on a solid substrate the lubrication pressure leads to the formation of a dimple at the base of the drop. These calculations are consistent with experimental observations of a trapped bubble for drop impact on a solid surface (Chandra & Avedisian 1991; Driscoll & Nagel 2011; van der Veen *et al.* 2012; Kolinski *et al.* 2012). Extrapolating these results to the case of drop impact on a liquid substrate suggests that the trapped disk of air observed by Thoroddsen *et al.* (2003) and in our experiments is caused by the same mechanism: the lubrication pressure of the surrounding gas causing a local deformation of the liquid surfaces.

We measured the initial size of the disk for all three liquids at various impact speeds. In these experiments the impact was viewed from directly below through the liquid and container, both of which were transparent. The disk shrinks within ≈ 30 μs by an order of magnitude to form a spherical bubble. In order to identify the initial radius of the disk, we filmed multiple impact events for the same experimental conditions at 210,000 frames-per-second, measured the radius of the disk for each event from the first video frame in which it appears (i.e. when it is largest), and selected the largest of these as the initial disk size R_b. The typical size of R_b is 2×10^{-2} cm which is consistent with magnitude expected from balancing lubrication pressure and inertia (see appendix).

The disk radius normalized by the drop radius are plotted in Fig. 4 versus Stokes number $St = \eta_g/\rho U D$. The data for all liquids collapses to a single curve in agreement with the scaling based on the Stokes number predicted in the dry impact problem (Mandre *et al.* 2009; Duchemin & Josserand 2011). Though we find $R_b \sim St^{0.5}$, our data covers less than a decade and thus the difference in our measured exponent and the 1/3 of Mandre *et al.* (2009); Duchemin & Josserand (2011) is not significant. Since $St = \Lambda/Re$, these data show that R_b increases with Λ. Moreover, the magnitude of the bubble size is consistent with a balance of the lubrication pressure and inertia.

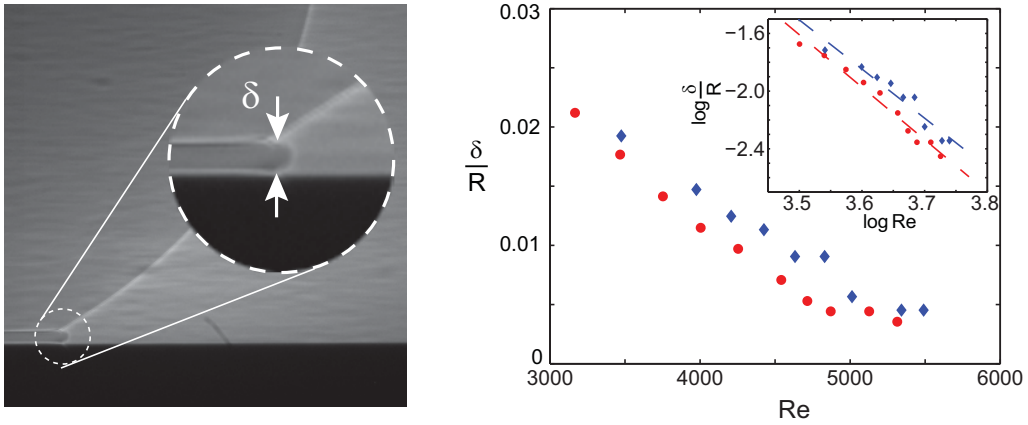

FIGURE 5. Left: Example of ejecta thickness measurement. Right: thickness of ejecta sheet normalized by the drop radius versus Reynolds number for GW (circles) and SO (diamonds). Note: the thickness is systematically larger for SO than GW at the same Re. Inset: same data plotted on a log-log scale. Dashed lines are best f its to a power law ARe^{α} which yield $A = 0.25 \times 10^{11}$ and $\alpha = -3.4$ for SO and $A = 1.3 \times 10^{11}$ and $\alpha = -3.6$ for SO.

3.4. *Connection between gas disk and ejecta*

The scaling of the disk radius with Λ suggests a connection between the gas disk and the evolution of the ejecta. Certainly it is plausible that if the gas is interfering with the merger of the drop and the pool, the ejecta would be affected. We speculate on how this might influence the threshold for the instability on the ejecta.

Increasing the gas viscosity increases the size of the trapped disk as demonstrated by our measurements. A bigger disk means that point of first contact between the drop and the pool is pushed further from the center. From volume conservation we expect that a bigger area of first contact will lead to a thicker ejecta: the outflow through the ejecta $2\pi R_b \delta u_j$ must balance the inflow from the drop $\pi R_b^2 U$, and thus $\delta u_j = R_b U/2$.

While in principle either δ or u_j could compensate for an increase in R_b, in practice we find that the ejecta thickens. We measured the ejecta's thickness when it first emerges from the neck connecting the drop and the pool. An example of this is shown in Fig. 5(a). The precision of this measurement is limited at 10% by pixelation. The thickness of the tip of the ejecta varied by less than 10% in subsequent frames (20 μs apart) in accord with the limited Taylor-Culick contraction expect at these short timescales. The thickness data is plotted in Fig. 5(b) versus Re. These data show that the ejecta is systematically thicker at all Re for the liquid with the bigger R_b, i.e. SO.

To complete the argument we assume that the instability is caused by capillarity as in the case of the crown splash Zhang *et al.* (2010). This assumption is consistent with the timescale at which we observe the appearance of the instability: the inverse growth rate for the Rayleigh-Plateau instability in non-dimensional time units is $\sqrt{We(\delta/R)^3}$ and is ≈ 1. Taylor-Culick contraction will cause the rim of a thicker ejecta to grow faster and it would thus be less susceptible to a Rayleigh-Plateau instability. In summary: higher gas viscosity produces a bigger disk; a bigger disk produces a thicker ejecta; and a thicker ejecta is more stable.

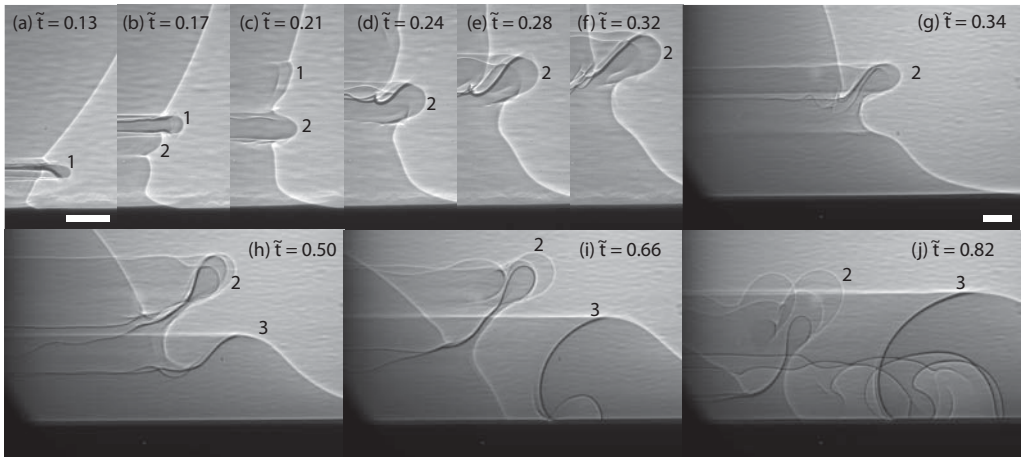

FIGURE 6. X-Ray phase contrast images showing ejecta (1), secondary ejecta (2) and lamella (3) of GW splash at $We = 230$, $Re = 4540$ with scaled time $\tilde{t} = Ut/D$. The scales bars in (a) and (g) equal 100 μm. The sequences (a-f) and (g-j) are from different impact events with the same experimental conditions. Note: the primary ejecta sheet is present in only the first two frames before being absorbed into drop between frame (b) and (c) leaving the ripples on the drop surface visible in (c). The lamella comes out much later in frame (h).

3.5. *Multiplicity of jets*

The splash in Fig. 1 shows two distinctly sized sets of secondary droplets. Neither set of droplets are due to the lamella which at that time is just beginning to rise from the pool. X-Ray images in Fig. 6 show two distinct jets from which the two sets of droplets detach. The first to appear and smaller set of droplets visible in Fig. 1 are the result of the disintegration of the ejecta labeled with the numeral "1" in Fig. 6. (At Re=4540 the impact event in Fig. 6 is below the splashing threshold and thus the jets do not break up.) The second set of droplets emerge later and come from the disintegration of a second jet, labeled with the numeral "2" in Fig. 6. Long after this second jet has emerged, the lamella begins to form. Hence, the second jet is distinct from both the ejecta and the lamella.

4. Conclusions

We conducted experiments of drop impact into a deep pool of the same liquid with three different liquids at the same We and Re in the high-Re/low-We regime. We demonstrated that the conventional scaling based on Re and We is insufficient to predict either the threshold for the generation of secondary droplets or the threshold for the instability which leads to the production of secondary droplets . Though the density of the surrounding gas seemed a likely candidate to explain the observed deviations based on previous results Xu *et al.* (2005), our experiments show that the effect of density is negligible. Instead our experiments show that the ratio of the dynamic viscosity of the gas and the liquid correlates well with the observed shift in the splashing threshold. We proposed that the disk trapped between the drop and the pool when these merge is responsible for this shift. We also discovered a third jet, distinct from the ejecta and lamella, which produces droplets of intermediate size to those from the ejecta and lamella.

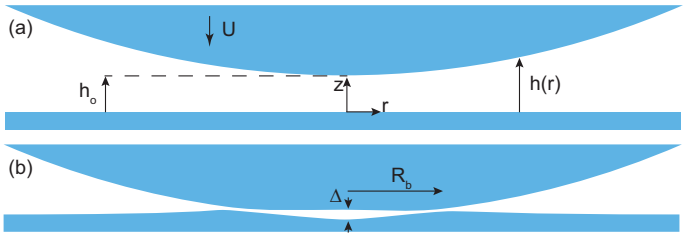

FIGURE 7. Schematic of the gap as the drop approaches the pool when (a) the drop is far from pool and (b) the air squeezed between the two bodies causes the interfaces to distort.

Appendix A

We estimate the radius of disk of gas trapped between the drop and the pool by balancing the inertial and lubrication forces. Consider the flow in the gap between the drop and the pool shown in Fig. 7(a). The lubrication equations (Batchelor 2000) are

$$\partial_r p \approx \eta_g \partial_z^2 u \tag{A 1}$$

$$\partial_z p \approx 0 \tag{A 2}$$

where r and z are the radial and vertical coordinates defined in Fig. 7(a), $u(r,z)$ is radial velocity component of the gas, and p is the pressure. Solving for p and using volume conservation yields

$$p = 6\eta_g U \int_r^\infty \frac{r dr}{h^3} \tag{A 3}$$

Approximating the gap profile with a parabola $h \approx h_o + \frac{1}{2}\frac{r^2}{R}$, the pressure at r is

$$p(r) = \frac{3\eta_g U R}{\left(h_o + \frac{1}{2}\frac{r^2}{R}\right)^2} \tag{A 4}$$

and the lubrication force F_L over a patch of size R_b when $h_o = \Delta$ is

$$F_L = 3\pi\eta_g U R \left(\frac{R_b}{\Delta}\right)^2 \frac{1}{1 + \frac{1}{2}\frac{R_b^2}{R\Delta}} \tag{A 5}$$

Balancing the work by this force against the change in kinetic energy of the fluid pushed aside by the gas yields

$$\frac{1}{2}\rho R_b^2 \Delta \, U^2 = F_L \Delta \tag{A 6}$$

and after rearrangement

$$R_b^2 \Delta = 12\pi St R^3 \tag{A 7}$$

The radius of the disk radius shrinks by a factor of ten as it contracts into a spherical bubble. Assuming the volume of the gas is conserved, we estimate $\Delta \approx 10^{-3} R_b$. Using $R = 0.1$ cm and $St = 5 \times 10^{-6}$, gives $R_b = 6 \times 10^{-2}$ cm in fair agreement with the typical measured value of 2×10^{-2} cm.

We thank Claudio Falcón for assistance with the measurements, and Michael Brenner for discussions. Use of the Advanced Photon Source, an Office of Science User Facility operated for the U.S. Department of Energy (DOE) Office of Science by Argonne National Laboratory, was supported by the U.S. DOE under Contract No. DE-AC02-06CH11357. RDD acknowledges support from the James S. McDonnell Foundation 21st Century Science Initiative in Studying Complex Systems-Research Award.

REFERENCES

Batchelor, G. K. 2000 *An introduction to fluid dynamics*. Cambridge University Press.

Chandra, S. & Avedisian, C. T. 1991 On the collision of a droplet with a solid-surface. *Proceedings of the Royal Society of London Series a-Mathematical Physical and Engineering Sciences* **432** (1884), 13–41.

Cossali, G. E., Coghe, A. & Marengo, M. 1997 Impact of a single drop on a wetted solid surface. *Experiments in Fluids* **22** (6), 463–472.

Deegan, R. D., Brunet, P. & Eggers, J. 2008 Complexities of splashing. *Nonlinearity* **21** (1), C1–C11.

Driscoll, Michelle M. & Nagel, Sidney R. 2011 Ultrafast interference imaging of air in splashing dynamics. *Physical Review Letters* **107**.

Duchemin, L. & Josserand, C. 2011 Curvature singularity and film-skating during drop impact. *Physics of Fluids* **23**, 091701.

Fezzaa, K. & Wang, Y. J. 2008 Ultrafast x-ray phase-contrast imaging of the initial coalescence phase of two water droplets. *Physical Review Letters* **100**, 104501.

Kolinski, John M., Rubinstein, Shmuel M., Mandre, Shreyas, Brenner, Michael P., Weitz, David A. & Mahadevan, L. 2012 Skating on a film of air: Drops impacting on a surface. *Physical Review Letters* **108** (7).

Lemmon, E.W., Huber, M.L. & McLinden, M.O. 2010 Nist standard reference database 23: Reference fluid thermodynamic and transport properties.

Mandre, Shreyas, Mani, Madhav & Brenner, Michael P. 2009 Precursors to splashing of liquid droplets on a solid surface. *Physical Review Letters* **102**, 134502.

Rioboo, R., Bauthier, C., Conti, J., Voue, M. & De Coninck, J. 2003 Experimental investigation of splash and crown formation during single drop impact on wetted surfaces. *Experiments in Fluids* **35**, 648–652.

Smith, F. T., Li, L. & Wu, G. X. 2003 Air cushioning with a lubrication/inviscid balance. *Journal of Fluid Mechanics* **482**, 291–318.

Thoroddsen, S. T. 2002 The ejecta sheet generated by the impact of a drop. *Journal of Fluid Mechanics* **451**, 373–381.

Thoroddsen, S. T., Etoh, T. G. & Takehara, K. 2003 Air entrapment under an impacting drop. *Journal of Fluid Mechanics* **478**, 125–134.

Thoroddsen, S. T., Thoraval, M. J., Takehara, K. & Etoh, T. G. 2011 Droplet splashing by a slingshot mechanism. *Physical Review Letters* **106**, 034501.

van der Veen, Roeland C. A., Tuan, Tran, Lohse, Detlef & Sun, Chao 2012 Direct measurements of air layer profiles under impacting droplets using high-speed color interferometry. *Physical Review E* **85**, 026315.

Weiss, D. A. & Yarin, A. L. 1999 Single drop impact onto liquid films: neck distortion, jetting, tiny bubble entrainment, and crown formation. *Journal of Fluid Mechanics* **385**, 229–254.

Worthington, A. M. 1882 On impact with a liquid surface. *Proc. Phys. Soc. London* **34**, 217–230.

Xu, L. 2010 Instability development of a viscous liquid drop impacting a smooth substrate. *Physical Review E* **82**, 025303.

Xu, L., Zhang, W. W. & Nagel, S. R. 2005 Drop splashing on a dry smooth surface. *Physical Review Letters* **94**, 184505.

Zhang, L. V., Brunet, P., Eggers, J. & Deegan, R. D. 2010 Wavelength selection in the crown splash. *Physics of Fluids* **22**, 122105.

Zhang, L. V., Toole, J., Fezzaa, K. & Deegan, R. D. 2012 Evolution of the ejecta sheet from the impact of a drop with a deep pool. *Journal of Fluid Mechanics* **690**, 5.